Hydrogen and Helium atoms in intense magnetic fields coupled with high pressure in neutron star atmospheres

Anand Thirumalai*

Department of Physics, DigiPen Institute of Technology, 9931 Willows Road NE, Redmond, WA, USA, 98052

E-mail: anandt@digipen.edu

Phone: +1(425)629 4442. Fax: +1(425)558 0299

Abstract

In addition to harboring intense global magnetic fields, neutron stars also have outer envelopes that are subject to high pressures. The outermost layer of a neutron star's envelope consists of a thin atmosphere, which in turn sits atop an ocean layer of condensed matter. The pressure at the topmost layer of the ocean is generally estimated to be around $P \gtrsim 10^3$ GPa. The envelope is thought to be dynamic, with mixing between the layers and this investigation seeks to delineate the energy landscape of neutral atoms from the atmosphere which can get trapped inside denser surrounding material of the ocean layer below during mixing. The high pressure environment is modelled as a quantum confined model by means of a spherical cavity; using a piecewise potential (V_p) and a confinig radius (R_C). A range of pressures and magnetic field strengths ($\sim 10^{6-9}$ T) are considered and the two most astrophysically relevant atoms (hydrogen and helium) are studied herein and, to the best of the author's knowledge, this is the first study to investigate the combination of the two effects in neutron star atmospheres. The energies of the first few low-lying states of each of hydrogen and helium atoms are computed (at the Hartree-Fock level of the theory for the latter) and the findings indicate that the binding energies of the states are considerably altered in such an environment. At the pressures relevant to the ocean layer ($P \gtrsim 10^3$ GPa), it was found that the negative parity states of both hydrogen and helium do not survive as the energy shift introduced by the confinement is large enough to render them unbound. The positive parity states of these atoms do however survive at such pressures (albeit with somewhat lesser binding energies, for the case of helium), in neutron star envelopes. At lower pressures $P \sim 10^2$ GPa, representing material in the lower reaches of the atmoshere though not at ocean layer depths, the energy landcape is still found to be appreciably altered, for both the positive and the negative parity states of hydrogen and helium. Higher in the atmosphere, the energy shifts were found to diminish to negligible amounts for pressures relevant to the photosphere of the neutron star $P \sim 10^{-1}$ GPa. Overall, the study reveals that incorporating the effect of high pressure is important when studying the structure of atoms in the intense magnetic fields present in

neutron star envelopes, as significant shifts in the computed energies will have bearing on any subsequent computations of oscillator strengths, transition wavelengths as well as calculations of relative abundance of atoms and ions in atmosphere models. Thus the results are relevant to understanding the spectra of neutron stars.

1 Introduction

Neutron stars are the end product of stellar evolution of some of the most massive stars in the Universe. Ever since their discovery over fifty years ago, it has been clear that they are extreme objects harboring the most intense magnetic fields in the observable Universe.[1,2] As such, they represent unique astrophysical laboratories to study matter under extreme conditions. The most commonly observed neutron stars are pulsars and even run-of-the-mill pulsars (radio pulsars) can harbor intense magnetic fields on the order of $10^7 - 10^9$ T.[3] There exist even more strongly magnetized neutron stars called magnetars, which can have magnetic field strengths in excess of 10^9 T. Some magnetized white dwarfs posess somewhat weaker but nevertheless still strong magnetic fields, with strengths in the range $10^2 - 10^5$ T.[3] Even at these somewhat lower white dwarf field strengths, a Zeeman-type perturbative treatment of the field is not accurate.[3] For neutron star field strengths the structure of atoms is so strongly altered from the low-field case that expanding the wave function of the electron using a spherical basis set becomes a poor approximation. The atmospheres of neutron stars are predominantly composed of hydrogen and helium atoms,[4] however from recent X-Ray observations it has emerged that mid-Z atoms are also present, in particular carbon,[5] which is, cosmo-chemically speaking, one of the most important elements to be able to detect in any astrophysical context. It is generally expected that presence of lighter atoms in particular carbon in neutron star atmospheres is a signature of accretion of material surrounding the neutron star or from a companion star.[4] Therefore the study of low- and mid-Z atoms in neutron star atmospheres is essential to understaning the chemical composition of not only the neutron star itself, but also of the progenitor, as well as the circumstellar environment

prior to the supernova explosion itself.

A wealth of atomic data is required in order to be able to analyze neutron star spectra. The study of the energy landscape of atoms in neutron star atmospheres is but the first piece of the puzzle. Therefore over the past several years, numerous studies have examined the structure of low- and mid-Z atoms, ions and even molecules in neutron stars as well as in some highly magnetized white dwarfs,[6–64] with the majority focusing on the structure of light atoms. The reader is refered to a review article of atoms in strong and intense magnetic fields[65] and references therein for further reading. In the intense magnetic fields in neutron star atmospheres, the structure of atoms is remarkably changed with respect to low- and indeed, the field-free cases. An intense magentic field severely restricts the motion of the electrons in a direction perpendicular to the field and hence, spherical symmetry of the eigenstates are lost and the electron clouds in general become stretched out in the direction of the field. As a result the electron clouds assume shapes that become increasingly cigar- or pencil-like in their appearance[43,45,46] with increasing magnetic field strength. This restriction to the motion in the transverse direction with respect to the field results in the electron cloud becoming more localised in the vicinity of the positively charged nucleus and consequently, the electron becomes more tightly bound. In neutron star magnetic field strengths it becomes energetically favourable for the electron spins to anti-align with the magnetic field, resulting in fully spin-polarized (FSP) states becoming the dominant bound state configurations. This results in an open 'shell' structure, which is particularly stark for mid-Z atoms like carbon for example,[46] where the electrons occupy states with only a single electron in each 'shell'. Consequently, the energy landscape undergoes a remarkable change due to loss of symmetries; azimuthal symmetry becomes the predominant symmetry and the states are therefore better labelled using a completely different set of quantum numbers.[25–31] In intense magnetic fields states can be characterized using the notation $\nu^{2S+1}\mathrm{M}^{\pi_z}$, where $\mathrm{M} = \Sigma_i m_i$ is the total $z-$ component of angular momentum. The summation is over all the electrons in the atom. The quantum number ν counts the excitation level within a given

M−manifold and sub-space symmetry. The spin multiplicity is given in the usual way as $2S + 1$. Finally, the $z-$parity of the state is indicated using $\pi_z = \pm$, indicating positive or negative parity. As an example[43–46,65] , the ground state of the helium atom in run-of-the-mill neutron star atmospheres is $1^3(-1)^{+1}$, which would correspond to a field-free fully spin-polarized configuration given by $1s_0 2p_{-1}$ (see Table 1).

However, in addition to an intense magnetic field being present in neutron star atmospheres there are also present strong electric fields[66] and a high pressure environment in the outer envelope.[67] Both of these effects can further complicate the energy landscape of atoms in neutron star atmospheres.

The atmosphere of a neutron star is the outermost layer of the envelope of the star (see e.g. Fig 2.1 on Page 54 of Hansel et al.[68]) and, it is on the order of about 0.4 cm thick.[69] However, over this depth the density ranges from about $\sim 10^{-4}$ to ~ 1 g/cm^3.[69] The photosphere of the neutron star resides within the atmosphere and the fiducial density of this part of the atmosphere is around $\sim 10^{-2}$ g/cm^3.[69] The pressure in the envelope is in general also high; in the GBar range for run-of-the-mill neutron stars,[67,69] which is similar to high pressure environments in the deep interiors of gas giant planets such as Jupiter and Saturn and to a limited extent, accessible in the lab via diamond anvil cell (see for e.g. Bonitz et al.[70]). Therefore, studying atoms in neutron star atmospheres theoretically and spectroscopically is a viable route for studying atoms in extreme environments; an environment that in addition to being characterized by high pressure, simultaneously is highly dense, has a high temperature (in excess of 10^6 K[68]) and also has a high magnetic field and a large electric field.[66] This confluence of extreme enrionmental conditions make neutron stars some of the most exteme environments in the observable universe.

The majority of studies of the structure of atoms in the extreme enviroments of neutron stars, have mainly focused on the intense magnetic field, or only a strong electric field, and in a handful of studies a combination of perhaps two environmental factors (see e.g. Tomczak and Pétri[66]). In this work the two extreme environmental factors combined are intense

magnetic fields and a high pressure environment; applicable to the lowermost layers of the atmosphere which are in contact and possibly mixing with a much denser 'ocean' layer of condensed matter underneath. The ocean layer is generally though to be composed of mid-Z atoms such as carbon, oxygen and iron.[71]

The problem of atoms subject to high pressures and confinement, is by itself a well established field of study.[72–76] Initial theoretical studies of confined atoms by Sommerfeld and Welker[77] laid the groundwork for modern day studies of atoms confined inside $2-D$ or $3-D$ structures; e.g. quantum dots[78] or, smaller atoms trapped inside the structures of larger ones like fullerenes[79] and also for experiments with diamond anvil cells for example[80] , that have explored novel physics and chemistry arising from matter being subjected to high pressures. The study of quantum dots subject to confinement in the presence of strong magnetic fields (up to a few tens of Tesla) is also a well established field with numerous investigations.[81–88] However, to the best of the author's knowledge however, there have not been any studies that have combined the effect of an intense magnetic field relevant to neutron stars ($B \gtrsim 10^{7-8}$ T) with a high pressure environment. In the outer envelope of a neutron star, the atmosphere and the ocean layer underneath it may mix[89] and, it may be possible for lighter material from the atmosphere to become trapped inside denser material at higher pressure. This would subject the lighter material to intense pressure and confinement, while still being subject to an intense magnetic field. This study represents an exploration of these implications on the energy landscape of the two most astrophysically relevant atoms (hydrogen and helium) and addresses an area of investigation that has thus far not been explored in the literature.

In the following section the theoretical framework is described. Following that the numerical details are briefly described, which is then followed by a discussion of the results. The study is then concluded with a summary of the findings alongside a discussion of its limitations and avenues for further work are discussed.

2 Theoretical Background

Since this is a preliminary investigation whose purpose is to ascertain whether including the effects of a high pressure environment is relevant for determining the structure of atoms in neutron star envelopes, the theory is restricted to a single-configuration Hartree-Fock (HF) formulation. This study utilizes a pseudospectral code developed for a series of earlier studies carried out by the author[44–46] and the reader is referred to a derivation of the single-configuration HF equation found therein. The numerical method for domain discretization using pseudospectral methods is also detailed in the above mentioned references. For the current study, the original pseudospectral code is modified to accommodate for an external potential representing the effect of a high pressure environment. Even though a detailed derivation and discussion of the numerical methods used can be obtained from the references mentioned above, a concise description of the theory and governing equations is repeated below from the author's prevous work for the sake of completeness.

Following Thirumalai and Heyl[45], the magnetic field is taken to be oriented along the $z-$direction and thus the single configuration HF equation can be written in cylindrical coordinates as [where the length scale is in units of Bohr radii (au) and the energy is scaled in units of Rydberg energy in the Coulomb potential of charge Ze ($E_{Z,\infty}$); see below for definitions],

$$\underbrace{\left[-\nabla_i^2(\rho_i,z_i)+\frac{m_i^2}{\rho_i^2}+2\beta_Z(m_i-1)+\beta_Z^2\rho_i^2-\frac{2}{r_i}+V_p\right]}_{H_{\rm hyd}}\psi_i\left(\rho_i,z_i\right)$$
$$+\frac{2}{Z}\sum_{j\neq i}\left[\Phi_D\psi_i(\rho_i,z_i)-\alpha_E\psi_j(\rho_i,z_i)\right]=\epsilon_i\psi_i\left(\rho_i,z_i\right), \qquad (1)$$

where $i,j=1,2,3,...,N$, where N is the number of electrons in the atoms, and $r_i=\sqrt{\rho_i^2+z_i^2}$. The wave function of a given configuration of electronic orbitals is assumed to be

given by a single Slater determinant as

$$\Phi = A_N \left(\tilde{\psi}_1, \tilde{\psi}_2, \tilde{\psi}_3, ..., \tilde{\psi}_{N-1}, \tilde{\psi}_N \right), \tag{2}$$

where A_N is the anti-symmetrization operator. The individual electronic wave functions $\tilde{\psi}_i$ are given by

$$\tilde{\psi}_i = \psi_i(\rho_i, z_i) e^{im\phi_i} \chi_i(s_i), \tag{3}$$

where i labels each of the N electrons. The two-dimensional spatial part of the single particle wave functions $\psi_i(\rho_i, z_i)$ are taken to be real functions. $\chi_i(s_i)$ are the spin parts of the wave functions. Please note that the three-dimensional Laplacian operator has been split into two parts: $\nabla_i^2(\rho_i, z_i)$ which are the $\rho-$ and $z-$ parts of the Laplacian; and m_i^2/ρ_i^2 which is the azimuthal part. The external potential due to the high pressure environment is taken to be of the form

$$V_p = \begin{cases} 0; & r_i \leq R_C \\ V_p; & r_i > R_C. \end{cases} \tag{4}$$

The external potential V_p and the confining radius R_C are both input parameters that are varied in the study. This then represents a rudimentary first approximation of the external high pressure environment that confines the atom. As mentioned earlier, the envelope of a neutron star consists of a thin atmosphere sitting atop an ocean layer of condensed matter. The ocean layer of a neutron star is generally thought to be barotropic with a top layer density of around ~ 1 g/cm^3.[69] Equation of state calculations for the envelopes of neutron stars yield pressures in the range of about $P \gtrsim 10^3$ GPa (see for e.g. Figure 1 of Nättilä et al.[69]) at the top layers of the ocean. Comparing this to the calculations shown in Figure 2 of Cabrera-Trujillo and Cruz[75] suggests that the confining radius must be small ($R_C \sim 1 - 2$ au) to attain such large pressures. Therefore in the current study, the smallest confining radius considered is about $R_C = 1$. We also consider as a point of comparison, the pressures that

would be present at around the fiducial density of the photosphere of around 10^{-2} g/cm^3 which corresponds to a pressure of about $P \sim 10^{-1}$ GPa.[69] Comparing this latter value of the pressure with calculations of Cabrera-Trujillo and Cruz[75] suggests that the confining radius must be around $R_C \sim 6$ au to sustain such pressures. Therefore in this exploratory study, three values of the confining radii are considererd due to the reasons mentioned above; $R_C = 1, 2,$ and 6 au. Furthermore, in their work Cabrera-Trujillo and Cruz[75] employed four different values of the confining potential, in the range $0 \leq V_p \leq \infty$; therefore in the current study, numerous values for V_p are employed in this same range. Together with the values of R_C mentioned above, it represents a quantum confinement that resembles a high pressure environment relevant to the outermost parts of neutron star envelopes; pressures in the range 0.1 GPa to $\gtrsim 10^3$ GPa.

It is to be mentioned that in cylindrical coordinates, the problem of a confined atom has been explored recently by Cabrera-Trujillo et al.[90],[91]. While they considered a confined hydrogen atom in cylindrical coordinates, they did not however consider an intense magnetic field as their focus was not neutron star atmospheres. Nevertheless the current study has similarities to their approach.

The total Hartree-Fock energy of the state is given as per the usual prescription according to,

$$\varepsilon_{total} = \sum_i \epsilon_i - \frac{1}{2}\frac{2}{Z}\sum_{j\neq i}\left[\langle\psi_i(\rho_i, z_i)|\Phi_D|\psi_i(\rho_i, z_i)\rangle - \langle\psi_i(\rho_i, z_i)|\alpha_E|\psi_j(\rho_i, z_i)\rangle\right]. \tag{5}$$

For the hydrogen atom, there are of course no direct and exchange potentials and hence, the Hamiltonian consists of merely the hydrogenic part, as labelled in Eq. 1. The direct (Φ_D) and exchange (α_E) interactions are determined according to the method outlined in Thirumalai and Heyl[43], as the solutions of the elliptic partial differential equations for the potentials given by

$$\nabla_i^2\Phi_D = -4\pi|\psi_j(\rho_i, z_i)|^2 \tag{6}$$

and

$$\left[\frac{1}{\rho_i}\frac{\partial}{\partial\rho_i}\left(\rho_i\frac{\partial}{\partial\rho_i}\right) - \frac{(m_i - m_j)^2}{\rho_i^2} + \frac{\partial^2}{\partial z_i^2}\right]\alpha_E(\rho_i, z_i) = -4\pi\psi_j^*(\rho_i, z_i)\psi_i(\rho_i, z_i). \tag{7}$$

Here ψ_i and ψ_j are the wave functions of the i^{th} and j^{th} electrons.

Integration with respect to the azimuthal coordinate, ϕ, has been carried out, prior to writing the result in Eq. (1) above. The contribution due to electron spin has also been averaged out *a priori*. It is to be mentioned in this regard that in the current study we shall only be concerned with FSP states; in other words all the electrons of the atom are assumed to be anti-aligned with the magnetic field. Such states have an exchange interaction between the electrons resulting in a coupling term in the HF equations; α_E and, FSP states are seen to be the most tightly bound states in the intense field regime.[43,45] The extension to partially spin-polarised configurations is easily achieved by eliminating the exchange term in the HF equations. In the current study, we shall work in units of Bohr radii along with the definitions given below.

The Bohr radius for an atom of nuclear charge Z is given by a_B/Z, where $a_B = \hbar/\alpha m_e c$ is the Bohr radius of the hydrogen atom. The magnetic field strength parameter β_Z, is given by the expression $\beta_Z = B/(Z^2 B_0)$, where B_0 is the critical field strength at which point the transition to the intense magnetic field regime occurs.[3] This is defined as $B_0 = (2\alpha^2 {m_e}^2 c^2)/(e\hbar) \approx 4.70108 \times 10^5$T. Thus, beyond a value of $\beta_Z \approx 1$, the interaction of the electron with the magnetic field gains dominance significantly as β_Z increases. Based upon the above definition of β_Z, it is convenient to classify the field strength[19] as low ($\beta_Z \leq 10^{-3}$), intermediate, also called strong ($10^{-3} \leq \beta_Z \leq 1$) and intense or high ($1 \leq \beta_Z \leq \infty$). These definitions of the different magnetic field strength regimes are useful to remember when discussing the results in the latter part of this paper and for distinguishing between "strong" and "intense" magnetic field strengths. The current study concerns itself with the *intense* magnetic field regime - the majority of neutron stars have magnetic fields of strength in this regime; typically $\beta_Z \gtrsim 100$ (see for example Fig. 1 in Gotthelf et al.[92]).

The energy parameter of the i^{th} electron is defined as $\epsilon_i = E_i/(Z^2 E_\infty)$, with $E_\infty =$

$\frac{1}{2}\alpha^2 m_e c^2$, the Rydberg energy of the hydrogen atom. For brevity we shall refer to the units of energy as $E_{Z,\infty}$, which should be remembered as the Rydberg energy in the Coulomb potential of charge Ze. The quantity $\alpha = e^2/(4\pi\epsilon_0\hbar c) \approx 1/137$ is the fine structure constant. In the current study, all the physical constants were used in SI units, with the magnetic field B in Tesla. Eq. (1) represents the N-coupled Hartree-Fock equations in partial differential form for an N-electron system with nuclear charge Z. The equations are coupled through the exchange interaction term between the electrons and as such the system of equations is solved iteratively. As mentioned before, the system of partial differential equations is solved using a pseudospectral approach and this has been detailed in the author's earlier studies.[45,46] A brief summary of the numerial method is given below and the reader is referred to the author's previous work mentioned above for further details.

3 Numerical Details

The HF equations given in Eq. 1 represent a coupled eigenvalue problem and its numerical solution proceeds via the so-called self-consistent field (SCF) method due to Hartree.[93] First we find a solution to the hydrogenic problem, without the direct and exchange interactions. This yields single electron hydrogenic wave functions in the Coulomb potential of charge Ze forming the initial estimates for the HF iterations. Second, using these estimates, the elliptic partial differential equations for the direct and exchange interaction potentials given in Eqs. 6 and 7 are solved (see Thirumalai and Heyl[45] for details). With these potentials now obtained, the coupled HF problem including the direct and exchange interactions is solved as an eigensystem. The exchange interactions that couple the equations are expressed using wave-functions from the previous iteration to solve the eigenvalue problem for each electron.[94] The eigenvalues obtained are the individual particle energies ϵ_i and the normalized eigenvectors are the wave functions, ψ_i. The SCF iterations then proceed with the updated electron wave functions and this process is repeated until convergence.

The confining potential due to an external pressure V_p is added to points in the domain which lie outside the confining radius, i.e.; $\sqrt{\rho^2 + z^2} > R_C$. To a first approximation this is a representation of an atom in a surrounding material that confines it. In the outermost layers of the envelope of a neutron star, this would represent a scenario wherein the material in the lower-most layers of the atmosphere finds itself surrounded by denser material from the ocean layer underneath.

For transforming the partial differential equations into algebraic ones, we follow the domain discretization procedure described in detail in Thirumalai and Heyl [45]. As a result of azimuthal symmetry of the problem, and parity with respect to the $z = 0$ plane, it is sufficient to restrict the physical domain of the problem [3,43,45] to $0 \leqslant \rho, z \leqslant \infty$. However, for making the problem numerically tractable, instead of using the above semi-infinite domain, we instead solve the problem in a finite albeit sufficiently large domain of size $\rho_{\max} \otimes z_{\max}$. This finite domain is then mapped using a suitable transformation (see below) to the domain $[-1, 1]$, and Chebyshev-Lobatto spectral collocation points are then located on this latter compactified domain. [95] Thereafter, a Chebyshev pseudospectral method can be employed for representing the differential operators and functions in this transformed domain. However, in order to mitigate errors due to domain truncation, computations were carried out on a sequence of domains of increasing sizes, obtaining a converged result in the limit of the computational domain approaching the size of the physical domain of the problem. [45]

In the current study, the size of the computational domain ($\rho_{\max}$ and $z_{\max}$ in units of Bohr radii) is given by

$$\rho_{\max} \ , \ z_{\max} = \frac{100\eta}{1 + \log_{10}(\beta_Z)}, \tag{8}$$

where $\eta = \frac{1}{2}, 1, 2$ is a scaling factor used for setting up computations in a sequence of increasing domain sizes. The effect of the logarithmic term $\log_{10}(\beta_Z)$ in the denominator is that it naturally makes the domain larger or smaller, depending on whether $\beta_Z < 1$ or $\beta_Z > 1$, respectively. With the maximum domain size thus defined, the finite domain is then

compactified as: $[0, \rho_{\max}] \otimes [0, z_{\max}]$ to $[-1, 1] \otimes [-1, 1]$ with the transformation,

$$x = \log_{10}(1 + \rho\alpha_\rho) - 1; \quad \forall\ x \in [-1, 1] \tag{9}$$

and

$$y = \log_{10}(1 + z\alpha_z) - 1, ; \quad \forall\ y \in [-1, 1], \tag{10}$$

where $\alpha_\rho = 99/\rho_{\max}$ and $\alpha_z = 99/z_{\max}$. In this study a square domain is employed for achieving the best possible internally consistent convergence. Therefore in the current work $\rho_{\max} = z_{\max}$ and consequently $\alpha_\rho = \alpha_z$, but the possibility remains for using different sizes and scalings in the two orthogonal directions for optimizing computational effort, particularly for $\beta_Z \gtrsim 200$, beyond which point the structure of the atom becomes increasingly extreme; cigar- or pencil-shaped and stretched out along the magnetic field. Boundary conditions employed are at the inner and outer boundaries of the compactified domain. In general, the wave function must vanish at the outer boudaries; reproduced by a Dirichlet boundary condition, while along the inner boudaries, depending on the azimuthal quantum number and the $z-$parity of the state, either a Dirichlet or Neumann condition is imposed. The reader is referred to Thirumalai and Heyl [45] for details on the method by which these conditions are applied within the framework of a pseudospectral method for the different states considered.

In order to obtain a converged solution within any given domain size, four different levels of mesh refinement were employed; using $N_g = 41, 51, 61$ and 71, where N_g is the number of Chebyshev collocation points used in each of the two orthogonal directions. Utilizing a pseudospectral approach for discretization results in a sparse matrix for the coupled eigenvalue problem. [45] The pseudospectral code employs the widely used sparse matrix generalized eigensystem solver ARPACK, which utilizes the implicitly restarted Arnoldi method (IRAM) [96–99] for solution. The key advantage is that since the Hamiltonian matrix that we are solving only has a few bound state solutions, employing IRAM with the shift-invert algorithm [98] for computing only a portion of the spectrum saves considerable computational effort.

It was found that generating a Krylov subspace with about 250 basis vectors was sufficient for determining around 1 to 10 bound state eigenvalues in the vicinity of a given shift (σ). Runs were carried out for different values of the magnetic field strength parameter β_Z, in the range $100 \leq \beta_Z \leq 1000$, for the cylindrical pseudospectral code. A typical tolerance of around 10^{-10} was employed for the internal errors of ARPACK. It was observed during the runs that fast convergence was achieved; within about $3-6$ HF iterations. A convergence criterion for the HF iterations was employed wherein the difference between the HF energies for two consecutive iterations was tested. Typically, a tolerance on the order of $10^{-6}E_{Z,\infty}$ was employed. Once the HF iterations attained convergence for a given level of mesh refinement, the total Hartree-Fock energy of the state is obtained according to Eq. 5.

4 Results and Discussion

Using the methodology described above, computations were carried out for six low-lying states of hydrogen and five of helium. The states investigated in this study are labelled as given in Table 1.

Table 1: The different states of Hydrogen and Helium considered in this study, listed using both intense-field and field-free notation.

	Intense-field	Field-free
Hydrogen	$1^2(0)^+$	$1s_0$
	$1^2(0)^-$	$2p_0$
	$1^2(-1)^+$	$2p_{-1}$
	$1^2(-1)^-$	$3d_{-1}$
	$1^2(-2)^+$	$3d_{-2}$
	$1^2(-2)^-$	$4f_{-2}$
Helium	$1^3(0)^-$	$1s_02p_0$
	$1^3(-1)^+$	$1s_02p_{-1}$
	$1^3(-1)^-$	$1s_03d_{-1}$
	$1^3(-2)^+$	$1s_03d_{-2}$
	$1^3(-2)^-$	$1s_04f_{-2}$

Convergence is imposed as described in Thirumalai and Heyl[45], and this allows the

estimation of the energies for the tightly bound states in the intense field regime, in the limit of an infinite domain size and infinitely fine mesh. In the current study we only investigated the states of hydrogen for which the quantum number $\nu = 1$; and we leave the investigation of more excites states such as $2^2(0)^+$ (which corresponds to the state $2s_0$ in field-free notation) etc, for future studies. In the discussion below we will focus on each π_z subspace of the two atoms considered.

4.1 Hydrogen atom: $\pi_z = +1$ subspace

Figure 1 shows the converged results for the states with positive parity ($\pi_z = +1$) of the hydrogen atom. The plots show the variation in the energies of the states with the external potential V_p. Three different confining radii are considered; i.e., $R_C = 1, 2, 6$, in units of Bohr radii, alongside six different values of the magnetic field strength parameter, β. It is to be kept in mind that the average neutron star has a magnetic field strength of around $\beta \approx 1000$. It can be seen in Figure 1 that at the lower values of the magnetic field strength, the effect of a confining potential results in the states becoming less bound with increasing value of the confining potential, V_p. This positive energy shift in the energy decreases with increasing confining radius. It is also immediately evident upon inspecting Figure 1 that the more diffuse states ($1^2(-1)^+$ and $1^2(-2)^+$) are the ones that are more affected by the inclusion of the confining potential. The $1^2(0)^+$ state of the hydrogen atom is the global ground state in the intense magnetic field regime and, the effect of the confining potential is only appreciable at the lower field strengths considered; $\beta \lesssim 200$. As the magnetic field strength increases beyond about $\beta \gtrsim 500$ the effect of the confining potential is not significant in any of the positive parity states considered here. As the magnetic field becomes increasingly intense it imposes a significant restriction on the motion of the electrons in the transverse direction to the field, effectively *confining* the electron cloud to be concentrated around the magnetic axis and subsequently, the nuclear potential pulls the electrons closer, thus increasing the binding energy. The effect on the electron clouds is that they are *simultaneously* elongated along

the magnetic axis and restricted to a small region in the vicinity of the nucleus. Thus, for the lower values of the magnetic field strengths considered here ($\beta \lesssim 200$), it is immediately evident that the effect of the confining potential is more pronounced when the confining radius is smaller (i.e., $R_C = 1$). For the larger values of the confining radii considered ($R_C = 2$ and $R_C = 6$), the effect of confinement is much less pronounced in the presence of intense magnetic fields for the positive parity states of hydrogen. Therefore we can conclude that for neutron stars that have lower magnetization ($\beta \lesssim 200$), in particular radio pulsars with low magnetic fields, the effect of a confining potential is important, particularly for the excited positive states of hydrogen, as the energy shifts are appreciable. This energy shift, while still present in the ground state, is much less pronounced therein. For neutron stars that have higher magnetization on the other hand ($\beta \gtrsim 500$), the effect of a confining potential for the positive parity states of hydrogen is not seen to be appreciable.

Moreover, it can be seen (particularly for $R_C = 1$ and $\beta = 100, 125, 200$) that the energies of the states seem to asymptote to a given value as the confining potential approaches a large number ($\sim 10^4 - 10^5 E_\infty$). This asymptotic limit represents a scenario similar to imposing a hard boundary condition at R_C. Naturally this is more pronounced for smaller values of R_C and can be readily seen in the energies.

The energy shift caused by the high pressure environment varies with both the magnetic field strength and the external potential. For example at $\beta = 100$, focusing on the data for $R_C = 1$ (which would correspond to a pressure of about $P \gtrsim 10^3$ GPa), we can see that the positive shift in the ground state energy (with respect to the case without an external potential) varies from a vanishingly small amount for small values of the external potential, to about $\Delta \sim 2\%$, as the magnitude of the external potential increases. For the excited states $1^2(-1)^+$ and $1^2(-2)^+$, this positive energy shift varies from a vanishingly small amount to around $\Delta \sim 8\%$, with increasing magnitude of the potential V_p, for $R_c = 1$. This energy shift is only seen to be appreciable for $R_C = 1$, and for larger confining radii the change is uniformly negligible for the positive parity states, regardless of the magnetic field strength.

We shall now discuss the results from the computations for the negative parity states of hydrogen considered in this study.

4.2 Hydrogen atom: $\pi_z = -1$ subspace

Figure 2 shows the converged results for the states with negative parity ($\pi_z = -1$) of the hydrogen atom. The plots show the variation in the energies of the states with the external potential V_p. Three different confining radii are considered; i.e., $R_C = 1, 2, 6$, in units of Bohr radii, alongside six different values of the magnetic field strength parameter, β. In the intense magnetic field regime pertinent to neutron star atmospheres, the negative parity states of hydrogen considered herein have low binding energies ($-1.2\ E_\infty \lesssim E < 0$) and are more diffuse than their positive parity counterparts.[43–45] The intense magnetic field of a neutron star makes their geometry extreme; severely restricted in the transverse direction to the field while simultaneously stretched out along the field. This gives the states a pencil-like appearance particularly for $\beta \gtrsim 100$.

Upon inspecting Figure 2 it can be seen that the data for energies of the negative parity states appear truncated for $R_c = 1$ at around $V_p = 1$. These parameters would correspond to a high pressure environment of about $P \gtrsim 10^3$ GPa (c.f. Figure 2 of Cabrera-Trujillo and Cruz[75]). The energy shift that the confining potential in the range $0 < V_p \leq 1$ introduces for the negative parity states at a value of $R_C = 1$ is on the order of about $\Delta \sim 20 - 60\%$ relative to the $V_p = 0$ case. This is already a large change and these states were *not* found to be bound at $V_p = 2$. Hence the energy shift renders them unbound when $1 < V_p \leq 2$ for $R_c = 1$.

Examining the data for the states when $R_c = 2$ it can be seen that the effect of the confining potential is that the states become progressively less bound with increasing value of the confining potential, regardless of the magnetic field strength. The pressures that this would correspond to are in the range $10^2 \lesssim P \lesssim 10^3$ GPa (c.f. Figure 2 of Cabrera-Trujillo and Cruz[75]). It can be seen that the binding energies of the states each approach an asymptote

as V_p becomes large ($\sim 10^4 - 10^5$); resembling a hard boundary condition at $R_c = 2$. Over the entire range of confining potentials and radii considered, the energy shift for the states ranges from a small fraction of a percent to about $\Delta \lesssim 80\%$. This energy shift appears to be significant at all the magnetic field strengths considered here. However, for $R_C = 6$, the effect of the confining potential is negligible, regardless of the field strength for these states. This corresponds to a pressure in the vicinity of about $P \sim 10^{-1}$ GPa, resembling conditions in the photosphere and, we can conclude that ambient pressure environment is not high enough here to affect the energies of these states.

Given these findings we can conlcude that the negative parity states of hydrogen are particularly sensitive to a high pressure environment with large energy shifts when the confining radius is small; i.e. $R_c = 1, 2$. The change is particularly stark for $R_c = 1$, when the states are rendered unbound for $1 < V_p \leq 2$. Thus we can conclude that a high pressure environment is in general not conducive to these negative parity states of hydrogen in neutron star envelopes which are under high pressure with appreciable dynamic variations.[69,100] This will have significant consequences for the oscillator strengths and subsequently the emergent spectra from neutron stars. It will also impact the relative abundance of atoms in excited state configurations with respect to the ground state, affecting also the calculations of neutron star atmosphere models and calculations of the equation of state.

Furthermore, upon examining the plots of the energies it can be seen that there are level crossings. For example, inspecting the data for $R_c = 2$, we can see that the states $1^2(0)^-$ and the state $1^2(-1)^-$ undergo a level crossing between $200 < \beta < 500$. Similarly, when the confining potential is small (i.e., $V_p < 1$), there are a few level crossings between the states. Overall, this is not unsurprising given that many of the excited states undergo level crossings in intense magnetic fields.[45] This also warrants further investigation to delineate the full energy landscape of the hydrogen atom, when simultaneously subjected to an intense magnetic field and an external potential with a confining radius. In future studies the parameter space ($\{V_p, R_c\}$) may also be explored in much finer detail in order to determine

the exact regions of the parameter space at which point the different states become unbound depending upon the magnetic field strength. In addition, many more states would need to be investigated in future in order to gain a fuller picture of the energy landscape of the hydrogen atom in a high pressure environment in neutron star atmospheres with intense magnetic fields. We now turn our attention to the helium atom.

4.3 Helium atom: $\pi_z = +1$ subspace

Figure 3 shows the converged results for the states with positive parity ($\pi_z = +1$) of the helium atom. The plots show the variation in the energies of the states with the external potential V_p. Three different confining radii are considered; i.e., $R_C = 1, 2, 6$, in units of Bohr radii, alongside six different values of the magnetic field strength parameter, $\beta_Z = B/(Z^2 B_0)$ (see definitions above). It is to be remembered that the majority of neutron stars have magnetic fields in excess of $\beta_Z \gtrsim 100$. Moreover, the excited state $1^3(0)^+$ of helium was not computed in this study as its computation involves first finding trial hydrogenic wave functions for the states $1^2(0)^+$ and $2^2(0)^+$ of hydrogen for starting the HF iterations; and only low-lying states with $\nu = 1$ were considered in this study. Computing this excited state of helium is left for future studies.

We can see from Figure 3 that for the states $1^3(-1)^+$ and $1^3(-2)^+$ however, the effect of the external potential is most profound for $R_C = 1$. For the larger values of $R_C = 2, 6$, there does not appear to be a significant effect on the energies of these states; there is a small variation as V_p increases for the lower magnetic field strengths considered, however this rapidly becomes negligible beyond about $\beta_Z = 200$. It can also be seen that for each of the magnetic field strengths shown, for $R_C = 1$, as the external potential increases in value, the energies tend to converge to an asymptote; similar to the behaviour of the positive parity states of the hydrogen atom. Similarly, as the magnetic field strength increases, the effect of the external potential is less pronounced overall in shifting the energy; the more intense the magnetic field, the more severely it constrains the electrons to be close to the nucleus and

the magnetic axis, and the magnetic field becomes the dominant "confining" effect.

The shift in the energies relative to the case when $V_p = 0$ is most profound for $\beta_Z = 100$ and diminishes with increasing field strength. For example, focusing on the plot for $\beta_Z = 100$ and $R_C = 1$, for the positive parity state $1^3(-1)^+$ it can be see that energy shift varies from a vanishingly small amount for low values of V_p to about $\Delta \sim 7-8\%$ as V_p increases to large values. Meanwhile for the excited state $1^3(-2)^+$ this energy shift correspondingly varies from an amount that is vanishingly small for small values of V_p to about $\Delta \sim 11\%$ for large values of V_p. For larger values of β_Z these percentages are smaller but nevertheless still appreciable. Therefore the effect of a high pressure environment is quite significant for the postive parity states of the helium atom, including the state $1^3(-1)^+$, which is the ground state in intense magnetic fields.

In summary, Figure 3 shows that in the magnetized atmosphere of a neutron star, a high pressure environment subjecting the atom to an external potential and a confining radius has an appreciable effect when $R_C = 1$; including for the ground state $1^3(-1)^+$. This will have implications for transition wavelengths and oscillator strengths since the energy shift is on the order of several percent for the range of magnetic field strengths considered herein. In particular, the shift is largest when the magnetic field is around $\beta_Z = 100$; which is about the magnetic field strength of run-of-the-mill neutron stars.

We now turn our attention to the negative parity states of the helium atom.

4.4 Helium atom: $\pi_z = -1$ subspace

Figure 4 shows the converged results for the states with negative parity ($\pi_z = -1$) of the helium atom. The plots show the variation in the energies of the states with the external potential V_p. Three different confining radii are considered; i.e., $R_C = 1, 2, 6$, in units of Bohr radii, alongside six different values of the magnetic field strength parameter, β_Z. In intense magnetic fields the excited states of the helium atom that have negative z-parity are generally more diffuse than their corresponding positive parity counterparts. Bound state

solutions for these states were not obtained when the value of the external potential was greater than unity, i.e., $V_p > 1$, for the smallest confining radius considered; $R_c = 1$.

The SCF iterations proceed by first finding an initial trial solution for the wave functions which are obtained by solving the corresponding problem of the hydrogen atom in a given magnetic field strength and external potential. The negative parity states of helium considered here depend upon computation of the hydrogenic states (shown in Figure 2) to be used as trial wave functions. As seen earlier, these negative parity eigenstates of the hydrogen atom were not found to be bound for $V_p > 1$ when $R_c = 1$. These states are weakly bound and $V_p > 1$ with $R_c = 1$ results in a large enough positive energy shift to render these states unbound. As a result, the SCF iterations could not proceed for values of $V_p > 1$ for helium for $R_c = 1$. This range of the parameter space corresponds to a pressure of about $P \sim 10^3$ GPa (c.f. Figure 2 of Cabrera-Trujillo and Cruz[75]). For the data shown the energy shifts due to the confining potential when $R_c = 1$ range from a few percent to about $\Delta \sim 10\%$, thus altering the energy landscape considerably. This therefore implies that in neutron star envelopes the negative parity states of helium are sensitive to the confining potential and these states may not be bound at such high pressures.

We can see from Figure 4 that when the confining radius is slightly larger $R_c = 2$, corresponding to a lower pressure in the range of about $10^2 \lesssim P \lesssim 10^3$ GPa, the energies of the states are still significantly affected. The energy shift ranges from a few percent to about $\Delta \sim 5 - 6\%$. Similar to the states of hydrogen, the energies become less bound as the confining potential increases to large values in the range $V_p \sim 10^4 - 10^5$ and rises to an asymptote. The energies of the states for $R_c = 6$ are largely unaffected by the confining potential.

It can also be seen in Figure 4 that there are several level crossings, not only when $V_p < 1$, but also between $200 < \beta_Z \leq 700$. Again, this is unsurprising given the fact that for the helium atom in intense magnetic fields level crossings have been reported for excited states,[45,65] particularly for the higher end of the magnetic field strengths shown.

Nevertheless, even with the limited amount data shown in Figure 4, it is clear that for the excited negative parity states of helium, a high pressure environment; even with relatively small values of V_p, significantly affects the energy landscape of these states and will therefore drastically alter the transition wavelengths and oscillator strengths. Moreover, since the negative parity states are not found to bound for $V_p > 1$ for $R_c = 1$, representing the case when the pressures are high $P \gtrsim 10^3$ GPa, it can be concluded that, similar to the hydrogen atom, a high pressure environment is generally not conducive for these excited states in the ocean layer of neutron star envelopes, though they may be able to withstand lower pressures. As a result, the relative abundance of excited states with respect to the ground state will also be greatly altered due to the presence of a high pressure environment, and this will consequently impact atmosphere models that rely upon theoretical computations.

From the preceding discussion it is evident that in neutron star atmospheres it is important to consider the effect of high pressure coupled with an intense magnetic field to fully understand the electronic structure of atoms in this uniquely extreme environment.

In the following section the findings of the current study are summarized along with a brief discussion of limitations of the study and avenues for futher investigation.

5 Summary and Conslusions

The energy landscape of the first few low-lying states of astrophysically relevant atoms; hydrogen and helium, were explored in this study, when simultaneously subjected to an intense magnetic field and a high pressure environment. This study focuses on the lower most layer of the atmosphere of a neutron star that is in contact with a dense ocean layer underneath. The pressure at this depth is expected to be around $P \gtrsim 10^3$ GPa. This preliminary investigation explores the situation in which material from the atmosphere (atoms) get trapped inside dense material of the ocean layer, which exerts a pressure and confines the atoms.

As a rudimentary first approximation, the high pressure environment is modelled in a

simplistic manner; a potential V_p which is nonzero outside a certain confining radius R_C. This potential is added to the Hamiltonian and bound eigenstates are then determined in intense magnetic fields for hydrogen and helium. The question this study seeks to explore is whether the effect of a high pressure environment is at all important in neutron star atmospheres and whether it will alter the electronic structure appreciably.

A previously developed two dimensional Hartree-Fock pseudospectral code for atomic structure[45,46] was employed in this investigation. The problem is cast into cylindrical coordinates and solved numerically obtaining the energies (ϵ_i) and wave functions ($\psi_i(\rho, z)$) for each electron of the atom.

The findings of this study reveal that including the effect of a high pressure environment is quite important for studying atoms in neutron star atmospheres. An intense magnetic field tends to increase the binding energies of the states. It is seen that the presence of an external potential V_p which is nonzero beyond a confining radius of R_C, introduces an energy shift making the states less bound, thus competing with the effect of the magnetic field. Overall, this shift is in the range of $\Delta \lesssim 1 - 10\%$ for the positive parity states of hydrogen and helium and about $\Delta \lesssim 1 - 60\%$ for the negative parity states of these atoms. The largest shifts in the latter states of these atoms were found to be in the region of the parameter space where $V_p \gtrsim 1$ and $R_c = 1$, representing the pressure in the uppermost part of the ocean layer; $P \gtrsim 10^3$ GPa. The negative parity states tend to have lower binding energies in neutron stars atmospheres in general and, with the inclusion of a high pressure environment, these were found to *not* be bound at these pressures. These state can however survive in a part of the parameter space representing lower pressures of about $10^2 \lesssim P \lesssim 10^3$ GPa; essentially further up in the atmosphere. Therefore in neutron star envelopes, particularly in the deeper parts of the atmosphere close to the ocean layer, likely only the positive parity states survive. Furthermore, for hydrogen overall, the energy shift is more pronounced for lower magnetic field strengths relevant to radio pulsars with low magnetic fields, meanwhile for helium, the effect is found to be appreciable for even the run-of-the-mill neutron stars.

In summary, the energy landscape is seen to be considerably altered due to the presence of a high pressure environment; to a large enough extent to significantly impact transition wavelengths, oscillator strengths, as well as the relative abundance of atoms in excited states in neutron star envelope models and consequently the study of neutron star spectra.

It is to be mentioned that the code employed herein has certain limitations. First, computations are currently required to be carried out in a sequence of increasing finite domain sizes, with a sequence of increasing mesh refinements (grid points) within each domain size, so that a converged result for the energies may be obtained in the limit of the domain size becoming infinite with an infinitely fine mesh.[45] This adds a significant layer of computational complexity and overhead. The reader is referred to a discussion in Thirumalai and Heyl[45] of a possible way to circumvent this, in essence by monitoring the wave functions at the outer edges of the domain and requiring their values to fall below a certain threshold, while varying the domain size. While this may not be straightforward to implement within the framework of a pseudospectral approach, it would nevertheless make the computation more streamlined if implemented. Second, this is a preliminary study and therefore the energy landscape of only a handful of states of hydrogen and helium are explored here. Many more states would need to be studied with the parameter space explored in finer detail in both the potential and the confining radius, in order obtain a thorough understanding.

Third, future studies could also examine the effect of a high pressure environment on the carbon atom, which has recently also been discovered in the atmospheres of neutron stars. Since the outer elctrons reside in more diffuse states in carbon, it is possible that in a high pressure environment, many of these states may become unbound, thus significantly altering the currently known energy landscape of carbon in neutron star atmospheres. Fourth, in the current study only a simplistic spherically symmetric confining potential is considered as that is the starting point of the majority of models of the ocean of a neutron star;[100] however, other types of potentials and confining geometries can also be considered. Deeper in the neutron star, in the crust, it is possible to have stable long chains of condensed matter.[35–42]

There, it may be possible to investigate smaller atoms trapped in a volume surrounded by such chains, introducing a cylindrical confinement with a large magnetic field. Thus, many avenues for future work are possible with the inclusion of high pressure.

Fifth, the current work does not include relativistic corrections to the energies. For the magnetic-field strengths considered herein, the relativistic corrections to the energies were estimated using the scaling formula in Poszwa and Rutkowski [101]. Their results for the hydrogen atom were used for this purpose and the corrections were estimated to be on the order of $10^{-6}E_{Z,\infty}$. This was seen to be smaller than the numerical errors arising from convergence of the entire numerical method including the extrapolation to the limit of an infinite domain. Thus, relativistic corrections are important however it was not possible to account for them accurately in the current study. Moreover, as the magnetic field strength increases in the intense magnetic field regime, effects due to finite nuclear mass become relevant. In the current study, the mass of the nucleus is assumed to be infinite, and as such, a suitable correction has not been carried out. One way to account for the finite nuclear mass is to employ a scaling relationship wherein the energies determined at a certain magnetic field strength β_Z for an infinite nuclear mass, would be related to the corresponding binding energies for a finite nuclear mass at a different value of the magnetic field strength $\tilde{\beta}_Z$.[30]

Finally, since this study is a preliminary exploration of high pressure effects in neutron star atmospheres, results are obtained at merely the HF level of the theory. Electron correlation is indeed important and can contribute a correction to the energies of a few percent; its inclusion via a post-HF formulation is however left as an avenue for future work.

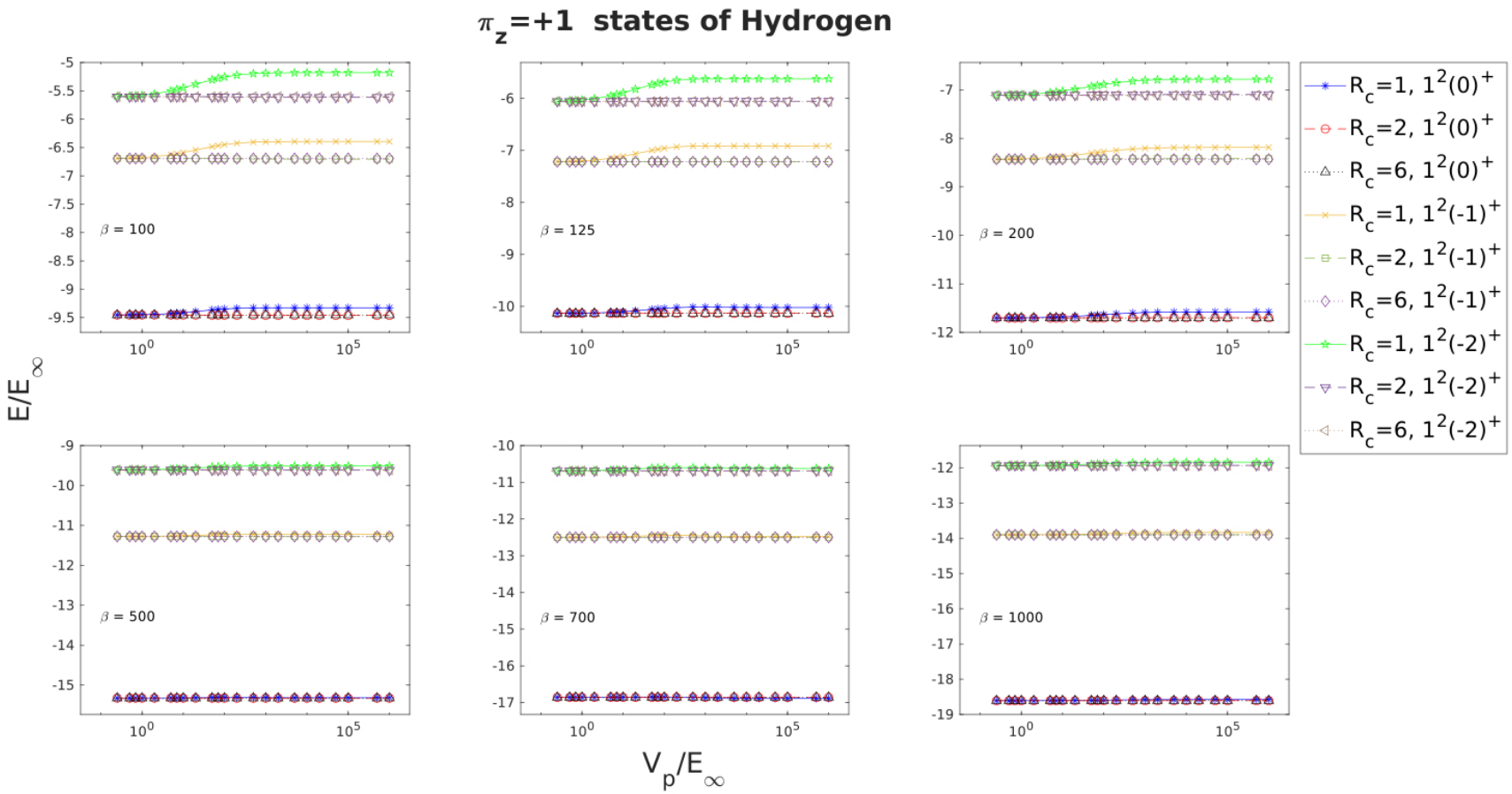

Figure 1: Variation in the energy of the $\pi_z = +1$ states of hydrogen as a function of the potential V_p. Shown are plots for three different confining radii, considered for six different values of the magnetic field strength parameter, β.

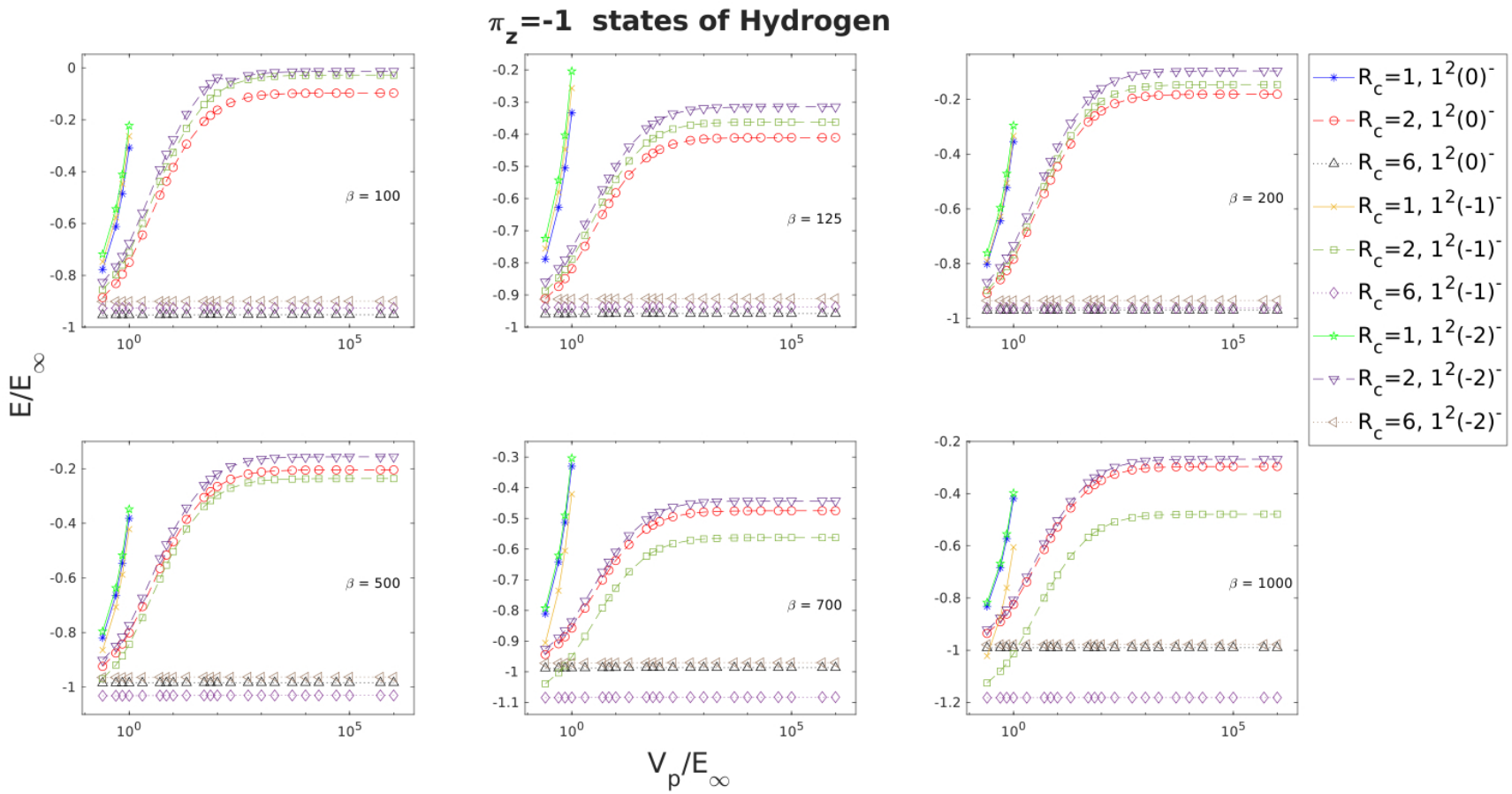

Figure 2: Variation in the energy of the $\pi_z = -1$ states of hydrogen as a function of the potential V_p. Shown are plots for three different confining radii, considered for six different values of the magnetic field strength parameter, β.

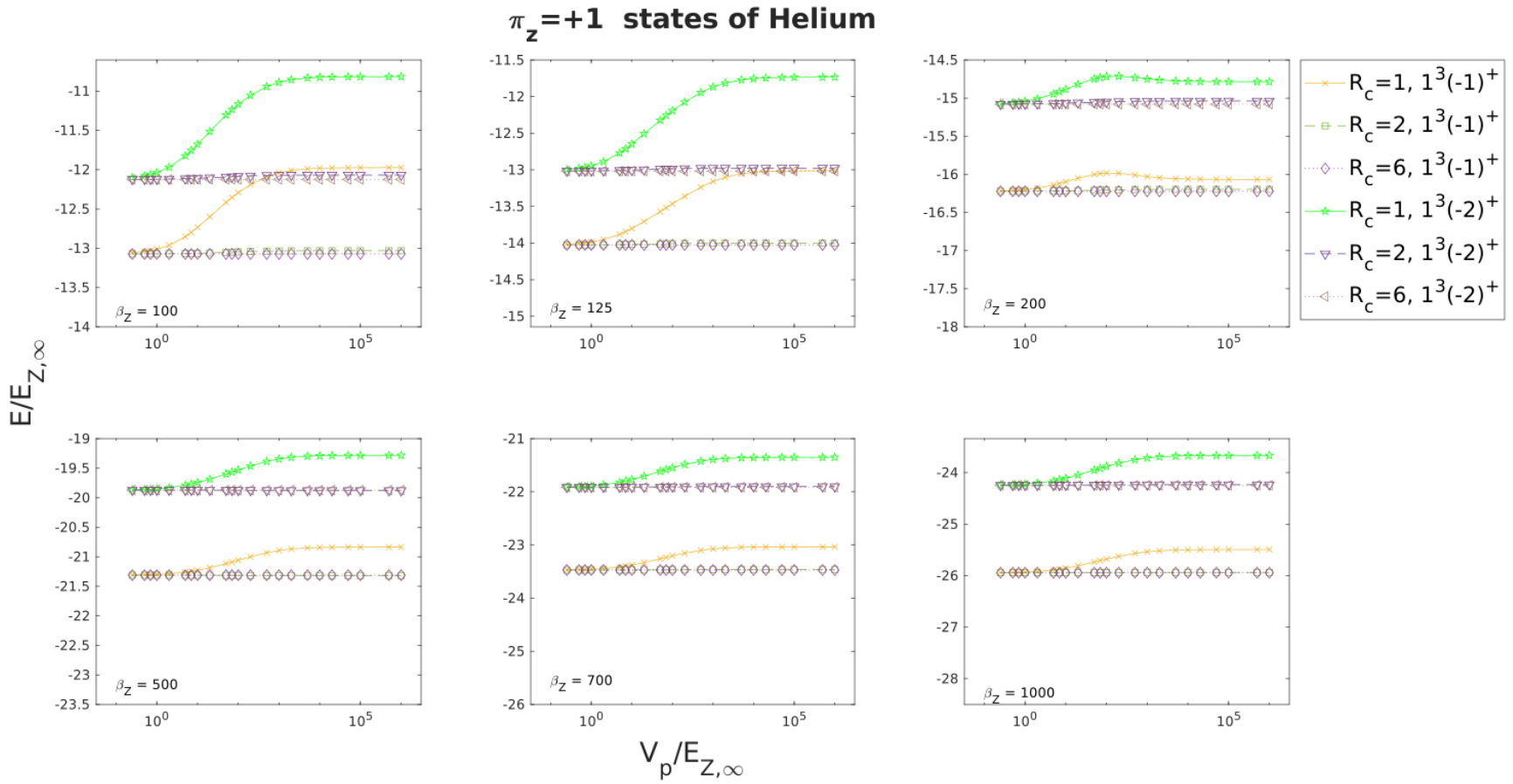

Figure 3: Variation in the energy of the $\pi_z = -1$ states of helium as a function of the potential V_p. Shown are plots for three different confining radii, considered for six different values of the magnetic field strength parameter, β_Z. The excited state $1^3(0)^+$ was not computed in this preliminary study (see discusison).

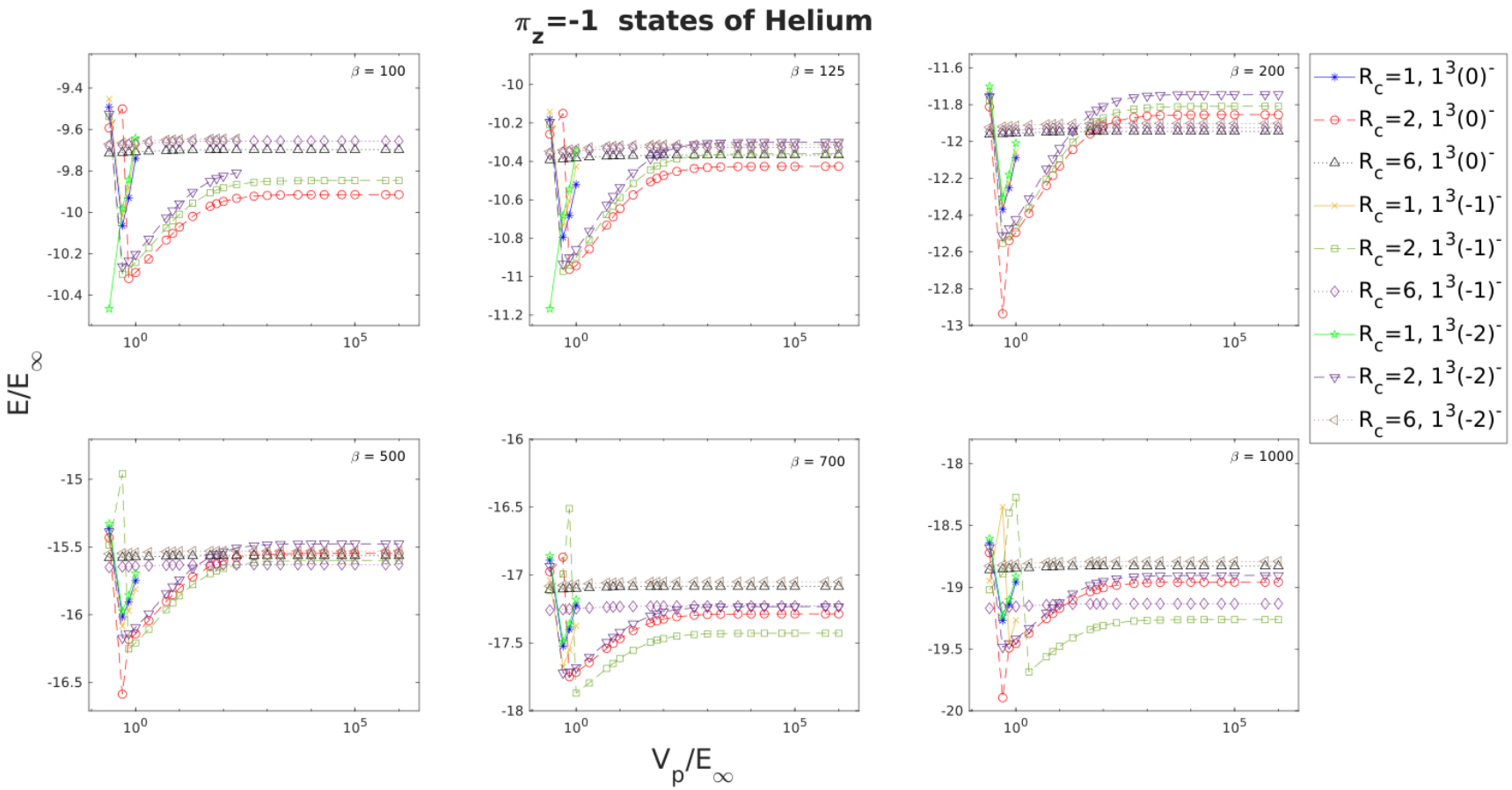

Figure 4: Variation in the energy of the $\pi_z = -1$ states of helium as a function of the potential V_p. Shown are plots for three different confining radii, considered for six different values of the magnetic field strength parameter, β_Z.

Acknowledgement

The author did not receive any financial support for this study. The author thanks the faculty and staff at the Hylleraas centre for Quantum Molecular Sciences at the University of Oslo for many fruitful discussions over the years and in particular Dr. Trygve Helgaker and Dr. Erik Tellgren.

References

(1) Trümper, J.; Pietsch, W.; Reppin, C.; Sacco, B.; Kendziorra, E.; Staubert, R. Evidence for Strong Cyclotron Emission in the Hard X-ray Spectrum of Her X-1. *Mitteilungen der Astronomischen Gesellschaft Hamburg* **1977**, *42*, 120.

(2) Truemper, J.; Pietsch, W.; Reppin, C.; Voges, W.; Staubert, R.; Kendziorra, E. Evidence for strong cyclotron line emission in the hard X-ray spectrum of Hercules X-1. *ApJ* **1978**, *219*, L105–L110.

(3) Ruder, H.; Wunner, G.; Herold, H.; Geyer, F. *Atoms in Strong Magnetic Fields: Quantum Mechanical Treatment and Applications in Astrophysics and Quantum Chaos*; Astronomy and Astrophysics Library; Springer-Verlag, New York, 1994.

(4) Salmi, T.; Vinciguerra, S.; Choudhury, D.; Watts, A. L.; Ho, W. C. G.; Guillot, S.; Kini, Y.; Dorsman, B.; Morsink, S. M.; Bogdanov, S. Atmospheric Effects on Neutron Star Parameter Constraints with NICER. *The Astrophysical Journal* **2023**, *956*, 138.

(5) Ho, W. C. G.; Heinke, C. O. A neutron star with a carbon atmosphere in the Cassiopeia A supernova remnant. *Nature* **2009**, *462*, 71–73.

(6) Canuto, V.; Kelly, D. C. Hydrogen Atom in Intense Magnetic Field. *ApSS* **1972**, *17*, 277.

(7) Praddaude, H. C. Energy Levels of Hydrogenlike Atoms in a Magnetic Field. *Phys. Rev. A* **1972**, *6*, 1321–1324.

(8) Simola, J.; Virtamo, J. Energy levels of hydrogen atoms in a strong magnetic field . *Journal of Physics B Atomic Molecular Physics* **1978**, *11*, 3309–3322.

(9) Friedrich, H. Bound-state spectrum of the hydrogen atom in strong magnetic fields. *Phys. Rev. A* **1982**, *26*, 1827–1838.

(10) Wunner, G.; Ruder, H. Lyman- and Balmer-like transitions for the hydrogen atom in strong magnetic fields. *Astron. & Astroph.* **1980**, *89*, 241–245.

(11) Roesner, W.; Herold, H.; Ruder, H.; Wunner, G. Approximate solution of the strongly magnetized hydrogenic problem with the use of an asymptotic property. *Phys. Rev. A* **1983**, *28*, 2071–2077.

(12) Roesner, W.; Wunner, G.; Herold, H.; Ruder, H. Hydrogen atoms in arbitrary magnetic fields. I - Energy levels and wavefunctions. *Journal of Physics B Atomic Molecular Physics* **1984**, *17*, 29–52.

(13) Ivanov, M. V. The hydrogen atom in a magnetic field of intermediate strength . *Journal of Physics B Atomic Molecular Physics* **1988**, *21*, 447–462.

(14) Baye, D.; Vincke, M.; Hesse, M. Simple and accurate calculations on a Lagrange mesh of the hydrogen atom in a magnetic field. *Journal of Physics B Atomic Molecular Physics* **2008**, *41*, 055005.

(15) Baye, D.; Hesse, M.; Vincke, M. The unexplained accuracy of the Lagrange-mesh method. *Phys. Rev. E* **2002**, *65*, 026701.

(16) Proeschel, P.; Roesner, W.; Wunner, G.; Ruder, H.; Herold, H. Hartree-Fock calculations for atoms in strong magnetic fields. I - Energy levels of two-electron systems. *Journal of Physics B Atomic Molecular Physics* **1982**, *15*, 1959–1976.

(17) Thurner, G.; Korbel, H.; Braun, M.; Herold, H.; Ruder, H.; Wunner, G. Hartree-Fock calculations for excited states of two-electron systems in strong magnetic fields . *Journal of Physics B Atomic Molecular Physics* **1993**, *26*, 4719–4750.

(18) Ivanov, M. V. Hartree-Fock mesh calculations of the energy levels of the helium atom in magnetic fields . *Journal of Physics B Atomic Molecular Physics* **1994**, *27*, 4513–4521.

(19) Jones, M. D.; Ortiz, G.; Ceperley, D. M. Hartree-Fock studies of atoms in strong magnetic fields. *Phys. Rev. A* **1996**, *54*, 219–231.

(20) Jones, M. D.; Ortiz, G.; Ceperley, D. M. Released-phase quantum Monte Carlo method. *Phys. Rev. E* **1997**, *55*, 6202–6210.

(21) Jones, M. D.; Ortiz, G.; Ceperley, D. M. Spectrum of neutral helium in strong magnetic fields. *Phys. Rev. A* **1999**, *59*, 2875–2885.

(22) Heyl, J. S.; Hernquist, L. Hydrogen and helium atoms and molecules in an intense magnetic field. *Phys. Rev. A* **1998**, *58*, 3567–3577.

(23) Mori, K.; Hailey, C. J. Atomic Calculation for the Atmospheres of Strongly Magnetized Neutron Stars. *ApJ* **2002**, *564*, 914–929.

(24) Mori, K.; Ho, W. C. G. Modelling mid-Z element atmospheres for strongly magnetized neutron stars. *MNRAS* **2007**, *377*, 905–919.

(25) Al-Hujaj, O.-A.; Schmelcher, P. Helium in superstrong magnetic fields. *Phys. Rev. A* **2003**, *67*, 023403.

(26) Al-Hujaj, O.-A.; Schmelcher, P. Electromagnetic transitions of the helium atom in superstrong magnetic fields. *Phys. Rev. A* **2003**, *68*, 053403.

(27) Becken, W.; Schmelcher, P. Electromagnetic transitions of the helium atom in a strong magnetic field. *Phys. Rev. A* **2002**, *65*, 033416.

(28) Becken, W.; Schmelcher, P. Higher-angular-momentum states of the helium atom in a strong magnetic field. *Phys. Rev. A* **2001**, *63*, 053412.

(29) Becken, W.; Schmelcher, P. Non-zero angular momentum states of the helium atom in a strong magnetic field . *Journal of Physics B Atomic Molecular Physics* **2000**, *33*, 545–568.

(30) Becken, W.; Schmelcher, P.; Diakonos, F. K. The helium atom in a strong magnetic field. *Journal of Physics B Atomic Molecular Physics* **1999**, *32*, 1557–1584.

(31) Luhr, A.; Al-Hujaj, O.-A.; Schmelcher, P. Resonances of the helium atom in a strong magnetic field. *Physical Review A (Atomic, Molecular, and Optical Physics)* **2007**, *75*, 013403.

(32) Ivanov, M. V.; Schmelcher, P. Ground state of the lithium atom in strong magnetic fields. *Phys. Rev. A* **1998**, *57*, 3793–3800.

(33) Ivanov, M. V.; Schmelcher, P. Ground states of H, He,..., Ne, and their singly positive ions in strong magnetic fields: The high-field regime. *Phys. Rev. A* **2000**, *61*, 022505.

(34) Wang, X.; Qiao, H. Configuration-interaction method with Hylleraas-Gaussian-type basis functions in cylindrical coordinates: Helium atom in a strong magnetic field. *Physical Review A (Atomic, Molecular, and Optical Physics)* **2008**, *77*, 043414.

(35) Lai, D.; Salpeter, E. E.; Shapiro, S. L. Hydrogen molecules and chains in a superstrong magnetic field. *Phys. Rev. A* **1992**, *45*, 4832–4847.

(36) Lai, D.; Salpeter, E. E.; Shapiro, S. L. Hydrogen Molecules and Chains in a Magnetic Neutron Star Atmosphere. Physics of Isolated Pulsars: proceedings of the Los Alamos Workshop, held in Taos, New Mexico, February 23-28, 1992. 1992; pp 160–167.

(37) Lai, D.; Salpeter, E. E. Hydrogen molecules in a superstrong magnetic field: Excitation levels. *Phys. Rev. A* **1996**, *53*, 152–167.

(38) Medin, Z.; Lai, D. Density-functional-theory calculations of matter in strong magnetic fields. I. Atoms and molecules. *Physical Review A (Atomic, Molecular, and Optical Physics)* **2006**, *74*, 062507.

(39) Medin, Z.; Lai, D. Density-functional-theory calculations of matter in strong magnetic fields. II. Infinite chains and condensed matter. *Physical Review A (Atomic, Molecular, and Optical Physics)* **2006**, *74*, 062508.

(40) Detmer, T.; Schmelcher, P.; Cederbaum, L. S. Hydrogen molecule in a magnetic field: The lowest states of the Π manifold and the global ground state of the parallel configuration. *Phys. Rev. A* **1998**, *57*, 1767–1777.

(41) Schmelcher, P.; Detmer, T.; Cederbaum, L. S. Excited states of the hydrogen molecule in magnetic fields: The singlet Σ states of the parallel configuration. *Phys. Rev. A* **2000**, *61*, 043411.

(42) Schmelcher, P.; Detmer, T.; Cederbaum, L. S. Excited states of the hydrogen molecule in magnetic fields: The triplet Σ states of the parallel configuration. *Phys. Rev. A* **2001**, *64*, 023410.

(43) Thirumalai, A.; Heyl, J. S. Hydrogen and helium atoms in strong magnetic fields. *Phys. Rev. A* **2009**, *79*, 012514.

(44) Heyl, J. S.; Thirumalai, A. Pseudo-spectral methods for atoms in strong magnetic fields. *MNRAS* **2010**, *407*, 590–598.

(45) Thirumalai, A.; Heyl, J. S. Two-dimensional pseudospectral Hartree-Fock method for low-Z atoms in intense magnetic fields. *Phys. Rev. A* **2014**, *89*, 052522.

(46) Thirumalai, A.; Desch, S. J.; Young, P. Carbon atom in intense magnetic fields. *Phys. Rev. A* **2014**, *90*, 052501.

(47) Ivanov, M. V. Hartree-Fock calculation of the $1s^2 2s^2$ state of the Be atom in external magnetic fields from γ=0 up to γ=1000. *Physics Letters A* **1998**, *239*, 72–80.

(48) Schmelcher, P.; Ivanov, M. V.; Becken, W. Exchange and correlation energies of ground states of atoms and molecules in strong magnetic fields. *Phys. Rev. A* **1999**, *59*, 3424–3431.

(49) Ivanov, M. V.; Schmelcher, P. Ground state of the carbon atom in strong magnetic fields. *Phys. Rev. A* **1999**, *60*, 3558–3568.

(50) Ivanov, M. V.; Schmelcher, P. The beryllium atom and beryllium positive ion in strong magnetic fields. *European Physical Journal D* **2001**, *14*, 279–288.

(51) Ivanov, M. V.; Schmelcher, P. The boron atom and boron positive ion in strong magnetic fields. *Journal of Physics B Atomic Molecular Physics* **2001**, *34*, 2031–2044.

(52) Engel, D.; Wunner, G. Hartree-Fock-Roothaan calculations for many-electron atoms and ions in neutron-star magnetic fields. *Phys. Rev. A* **2008**, *78*, 032515.

(53) Engel, D.; Klews, M.; Wunner, G. A fast parallel code for calculating energies and oscillator strengths of many-electron atoms at neutron star magnetic field strengths in adiabatic approximation. *Computer Physics Communications* **2009**, *180*, 302–311.

(54) Schimeczek, C.; Engel, D.; Wunner, G. A highly optimized code for calculating atomic data at neutron star magnetic field strengths using a doubly self-consistent Hartree-Fock-Roothaan method. *Computer Physics Communications* **2012**, *183*, 1502–1510.

(55) Schimeczek, C.; Boblest, S.; Meyer, D.; Wunner, G. Atomic ground states in strong magnetic fields: Electron configurations and energy levels. *Phys. Rev. A* **2013**, *88*, 012509.

(56) Klews, M.; Wunner, G.; Werner, K. Atomic Data for the Atmospheres of Strongly

Magnetized Neutron Stars. X-ray Diagnostics of Astrophysical Plasmas: Theory, Experiment, and Observation. 2005; pp 287–290.

(57) Boblest, S.; Schimeczek, C.; Wunner, G. Ground states of helium to neon and their ions in strong magnetic fields. *Phys. Rev. A* **2014**, *89*, 012505.

(58) Bücheler, S.; Engel, D.; Main, J.; Wunner, G. Quantum Monte Carlo studies of the ground states of heavy atoms in neutron-star magnetic fields. *Phys. Rev. A* **2007**, *76*, 032501.

(59) Bücheler, S.; Engel, D.; Main, J.; Wunner, G. Diffusion Monte Carlo Calculations for the Ground States of Atoms and Ions in Neutron Star Magnetic Fields. Path Integrals — New Trends and Perspectives. 2008; pp 315–320.

(60) Meyer, D.; Boblest, S.; Wunner, G. Fixed-phase correlation-function quantum Monte Carlo calculations for ground and excited states of helium in neutron-star magnetic fields. *Phys. Rev. A* **2013**, *87*, 032515.

(61) Austad, J.; Borgoo, A.; Tellgren, E. I.; Helgaker, T. Bonding in the helium dimer in strong magnetic fields: the role of spin and angular momentum. *Phys. Chem. Chem. Phys.* **2020**, *22*, 23502–23521.

(62) Hollands, M. A.; Stopkowicz, S.; Kitsaras, M.-P.; Hampe, F.; Blaschke, S.; Hermes, J. J. A DZ white dwarf with a 30 MG magnetic field. *Mon. Not. R. Astron. Soc* **2023**, *520*, 3560–3575.

(63) Kitsaras, M.-P.; Grazioli, L.; Stopkowicz, S. The approximate coupled-cluster methods CC2 and CC3 in a finite magnetic field. *J. Chem. Phys.* **2024**, *160*, 094112.

(64) Blaschke, S.; Kitsaras, M.-P.; Stopkowicz, S. Finite-field Cholesky decomposed coupled-cluster techniques (ff-CD-CC): theory and application to pressure broadening

of Mg by a He atmosphere and a strong magnetic field. *Phys. Chem. Chem. Phys.* **2024**, *26*, 28828–28848.

(65) Thirumalai, A.; Heyl, J. S. In *Chapter Five - Energy Levels of Light Atoms in Strong Magnetic Fields*; Arimondo, E., Berman, P. R., Lin, C. C., Eds.; Advances In Atomic, Molecular, and Optical Physics; Academic Press, 2014; Vol. 63; pp 323–358.

(66) Tomczak, I.; Pétri, J. Particle motion in ultra-strong electromagnetic fields of neutron stars: The influence of radiation reaction. *Astron. & Astroph.* **2023**, *676*, A128.

(67) Chabrier, G.; Douchin, F.; Potekhin, A. Y. Dense astrophysical plasmas. *Journal of Physics: Condensed Matter* **2002**, *14*, 9133–9139.

(68) Hansel, P.; Potekhin, A. Y.; Yakolev, D. G. *Neutron Stars 1: Equation of State and Structure*; Astronomy and Astrophysics Library; Springer New York, NY, 2007; Vol. 326; Chapter 2, p 54.

(69) Nättilä, J.; Cho, J. Y.-K.; Skinner, J. W.; Most, E. R.; Ripperda, B. Neutron Star Atmosphere–Ocean Dynamics. *The Astrophysical Journal* **2024**, *971*, 37.

(70) Bonitz, M.; Vorberger, J.; Bethkenhagen, M.; Böhme, M. P.; Ceperley, D. M.; Filinov, A.; Gawne, T.; Graziani, F.; Gregori, G.; Hamann, P. et al. Toward first principles-based simulations of dense hydrogen. *Physics of Plasmas* **2024**, *31*, 110501.

(71) Potekhin, A. Y.; Chabrier, G.; Yakovlev, D. G. Internal temperatures and cooling of neutron stars with accreted envelopes. *Astron. & Astroph.* **1997**, *323*, 415–428.

(72) Connerade, Jean-Patrick Confining and compressing the atom. *Eur. Phys. J. D* **2020**, *74*, 211.

(73) Sen, K. D., Ed. *Electronic Structure of Quantum Confined Atoms and Molecules*; Springer, 2014.

(74) *The Theory of Confined Quantum Systems, Parts I and II*; Advances in Quantum Chemistry; Academic Press, 2009; Vol. 57; pp 1–334.

(75) Cabrera-Trujillo, R.; Cruz, S. A. Confinement approach to pressure effects on the dipole and the generalized oscillator strength of atomic hydrogen. *Phys. Rev. A* **2013**, *87*, 012502.

(76) Reyes-García, R.; Cruz, S. A.; Cabrera-Trujillo, R. Heisenberg's uncertainty relations for a hydrogen atom confined by an impenetrable spherical cavity. *Phys. Rev. A* **2024**, *110*, 022814.

(77) Sommerfeld, A.; Welker, H. Künstliche Grenzbedingungen beim Keplerproblem. *Annalen der Physik* **1938**, *424*, 56–65.

(78) Kouwenhoven, L. P.; Austing, D. G.; Tarucha, S. Few-electron quantum dots. *Reports on Progress in Physics* **2001**, *64*, 701.

(79) Deshmukh, P. C.; Jose, J.; Varma, H. R.; Manson, S. T. Electronic structure and dynamics of confined atoms. *Eur. Phys. J. D* **2021**, *75*, 166.

(80) Deshmukh, P. C.; Jose, J.; Varma, H. R.; Manson, S. T. Thickness and Clapeyron slope of the post-perovskite boundary. *Nature* **2021**, *462*, 782–785.

(81) Maksym, P.; Chakraborty, T. Quantum dots in a magnetic field: Role of electron-electron interactions. *Physical review letters* **1990**, *65*, 108–111.

(82) Maniero, A.; Prudente, F.; de Carvalho, C.; Jalbert, G. 3D two-electron double quantum dot: Comparison between the behaviour of some physical quantities under two different confinement potentials in the presence of a magnetic field. *Physica B: Condensed Matter* **2023**, *657*, 414818.

(83) Nazmitdinov, R. G.; Simonović, N. S.; Plastino, A. R.; Chizhov, A. V. Shape transitions in excited states of two-electron quantum dots in a magnetic field. *Journal of Physics B: Atomic, Molecular and Optical Physics* **2012**, *45*, 205503.

(84) Simonović, N. S.; Nazmitdinov, R. G. Effect of the magnetic field on electron density distributions in two-electron quantum dots. *Journal of Physics A: Mathematical and Theoretical* **2019**, *52*, 435303.

(85) Nazmitdinov, R. G. Magnetic field and symmetry effects in small quantum dots. *Physics of Particles and Nuclei* **2009**, *40*, 71.

(86) Yannouleas, C.; Landman, U. Symmetry breaking and quantum correlations in finite systems: studies of quantum dots and ultracold Bose gases and related nuclear and chemical methods. *Reports on Progress in Physics* **2007**, *70*, 2067.

(87) Maksym, P. A. In *Atoms and Molecules in Strong External Fields*; Schmelcher, P., Schweizer, W., Eds.; Springer US: Boston, MA, 2002; pp 301–311.

(88) Hawrylak, P. Single-electron capacitance spectroscopy of few-electron artificial atoms in a magnetic field: Theory and experiment. *Phys. Rev. Lett.* **1993**, *71*, 3347–3350.

(89) Urpin, V. Neutron star oceans: Instability, mixing, and heat transport. *Astronomy and Astrophysics* **2004**, *421*, L5–L8.

(90) Cabrera-Trujillo, R.; Méndez-Fragoso, R.; Cruz, S. A. Energy-level structure of the hydrogen atom confined by a penetrable cylindrical cavity. *Journal of Physics B Atomic Molecular Physics* **2016**, *49*, 015005.

(91) Cabrera-Trujillo, R.; Méndez-Fragoso, R.; Cruz, S. A. Pressure effects on the dipole oscillator strength, polarizability, and mean excitation energy of a hydrogen impurity under cylindrical confinement: off-center axis effect. *Journal of Physics B Atomic Molecular Physics* **2017**, *50*, 135002.

(92) Gotthelf, E. V.; Halpern, J. P.; Allen, B.; Knispel, B. X-RAY OBSERVATIONS OF DISRUPTED RECYCLED PULSARS: NO REFUGE FOR ORPHANED CENTRAL COMPACT OBJECTS. *The Astrophysical Journal* **2013**, *773*, 141.

(93) Hartree, D. R. *The Calculation of Atomic Structures*; J. Wiley, New York, 1957.

(94) Slater, J. C. A Simplification of the Hartree-Fock Method. *Physical Review* **1951**, *81*, 385–390.

(95) Trefethen, L. N. *Spectral Methods in MATLAB*; Society for Industrial and Applied Mathematics, Philadelphia, Pennsylvania, 2000.

(96) Arnoldi, W. E. The principle of minimized iteration in the solution of the matrix eigenvalue problem. *Quart. J. Applied Mathematics, 9:17-29* **1951**,

(97) Sorensen, D. C. Implicit application of polynomial filters in a k-step Arnoldi method. *SIAM Journal of Matrix Analysis and Applications* **1992**, *13*, 357–385.

(98) Lehoucq, R. B.; Sorensen, D. C.; Yang, C. *ARPACK User's Guide*; SIAM, Philadelphia, 1998.

(99) Saad, Y. Chebyshev acceleration techniques for solving nonsymmetric eigenvalue problems. *Mathematics of Computation* **1984**, *42*, 567–588.

(100) Sullivan, A. G.; Alves, L. M. B.; Spence, G. O.; Leite, I. P.; Veske, D.; Bartos, I.; Márka, Z.; Márka, S. Multimessenger emission from tidal waves in neutron star oceans. *Monthly Notices of the Royal Astronomical Society* **2023**, *520*, 6173–6189.

(101) Poszwa, A.; Rutkowski, A. Hyrogen atom in a strong magnetic field. II. Relativistic corrections for low-lying states. *Phys. Rev. A* **2004**, *69*, 023403.

TOC graphic

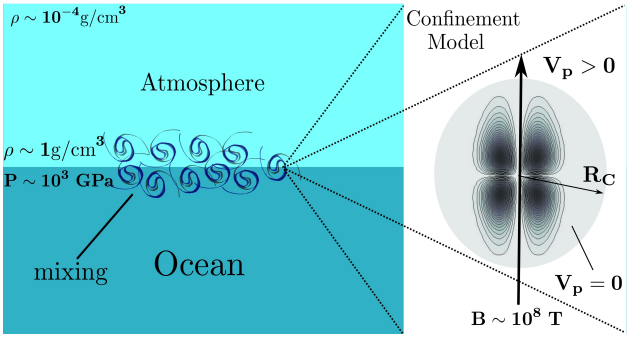
$\rho \sim 10^{-4}$g/cm^3
Atmosphere
$\rho \sim 1$g/cm^3
P $\sim 10^3$ GPa
mixing
Ocean
Confinement
Model
$V_P > 0$
R_C
$V_P = 0$
B $\sim 10^8$ T